Variation of phytoplankton assemblages along the Mozambique coast as revealed by HPLC and microscopy

Article *in* Journal of Sea Research · February 2013

DOI: 10.1016/j.seares.2013.01.001

CITATIONS
6

READS
255

8 authors, including:

Miguel Costa Leal
Eawag: Das Wasserforschungs-Institut des ET…
59 PUBLICATIONS **626** CITATIONS
SEE PROFILE

Alexandra Silva
Instituto Português do Mar e da Atmosfera
29 PUBLICATIONS **266** CITATIONS
SEE PROFILE

Jose Paula
University of Lisbon
104 PUBLICATIONS **2,034** CITATIONS
SEE PROFILE

Vanda Brotas
University of Lisbon
116 PUBLICATIONS **2,092** CITATIONS
SEE PROFILE

Journal of Sea Research 79 (2013) 1–11

Contents lists available at SciVerse ScienceDirect

Journal of Sea Research

journal homepage: www.elsevier.com/locate/seares

Variation of phytoplankton assemblages along the Mozambique coast as revealed by HPLC and microscopy

C. Sá [a,*], M.C. Leal [b,1], A. Silva [a], S. Nordez [c], E. André [c], J. Paula [b], V. Brotas [a,d]

[a] Centro de Oceanografia, Faculdade de Ciências, Universidade de Lisboa, Campo Grande, 1749-016 Lisboa, Portugal
[b] Centro de Oceanografia, Laboratório Marítimo da Guia, Faculdade de Ciências da Universidade de Lisboa, Av. Nª Senhora do Cabo, 939, 2759-374 Cascais, Portugal
[c] Instituto de Investigação Pesqueira de Moçambique, Av. Mao Tse-Tung no. 389, Maputo, C.P. 4603, Mozambique
[d] Plymouth Marine Laboratory, The Hoe, Plymouth PL1 3DH, United Kingdom

ARTICLE INFO

Article history:
Received 30 April 2012
Received in revised form 12 December 2012
Accepted 18 January 2013
Available online 4 February 2013

Keywords:
Phytoplankton
HPLC Pigments
Mozambique Channel
Agulhas Current
Indian Ocean

ABSTRACT

This study is an integrated overview of pigment and microscopic analysis of phytoplankton communities throughout the Mozambican coast. Collected samples revealed notable patterns of phytoplankton occurrence and distribution, with community structure changing between regions and sample depth. Pigment data showed Delagoa Bight, Sofala Bank and Angoche as the most productive regions throughout the sampled area. In general, micro-sized phytoplankton, particularly diatoms, were important contributors to biomass both at surface and sub-surface maximum (SSM) samples, although were almost absent in the northern stations. In contrast, nano- and pico-sized phytoplankton revealed opposing patterns. Picophytoplankton were most abundant at surface, as opposed to nanophytoplankton, which were more abundant at the SSM. Microphytoplankton were associated with cooler southern water masses, while picophytoplankton were related to warmer northern water masses. Nanophytoplankton were found to increase their contribution to biomass with increasing SSM. Microscopy information on the genera and species level revealed the diatoms *Chaetoceros* spp., *Proboscia alata*, *Pseudo-nitzschia* spp., *Cylindrotheca closterium* and *Hemiaulus haukii* as the most abundant taxa of the micro-sized phytoplankton. *Discosphaera tubifera* and *Emiliania huxleyi* were the most abundant coccolithophores, nano-sized phytoplankton.

1. Introduction

Mozambique is located in Southeast Africa and has a coastline of 2500 km covering a latitudinal range between 10°20′S and 26°50′S. Two water masses are usually identified in this large latitudinal gradient: the northern, predominantly Tropical Surface Water that is influenced by the warm equatorial branch of the South Equatorial Current (salinity<35.5), and the southern, mostly Subtropical Surface Water (with salinity greater than 35.5) derived from the center of the subtropical anti-cyclonic vortex of the Indian Ocean (Saetre and Da Silva (1982) in Gove, 1995). Oceanographic processes in the region are mainly influenced by the Agulhas Current system (Lutjeharms, 2006). This system consists of well-developed western boundary currents along the east coast of Madagascar and South Africa, and a series of mesoscale eddies through the Mozambique Channel heading south along the western shelf edge of Mozambique. De Ruijter et al. (2002) observed 4 to 5 anticyclonic eddies per year, which play an important local role in coastal and oceanographic processes (Lutjeharms, 2006). Some eddies promote upwelling, defined as the uplift of deeper nutrient richer waters, which increase surface water nutrient content and, therefore, enhance biomass concentration (cell number and chlorophyll-*a*; Chl *a*; Quartly and Srokosz, 2004). In addition to upwelling, meteorological conditions, tides and river runoff (e.g. Limpopo and Zambezi rivers) significantly influence the marine processes and ecosystems off the coast of Mozambique. These factors determine not only the biomass abundance distribution but also the occurrence of different planktonic communities (Leal et al., 2009, 2010).

Phytoplankton communities are essential to the majority of ecological processes and affect the structure of food webs (e.g., primary production), nutrient cycling and the flux of particles to deep waters. Its distribution changes both horizontally and vertically (Barlow et al., 2007; Brunet and Lizon, 2003; Leal et al., 2009). Locally, temperature, salinity and currents, along with other factors, determine the horizontal distribution, while vertical distribution is primarily determined by irradiance, nutrients and water column stability. The effect of these factors on phytoplankton abundance and community structure is known to vary among worldwide regions, from tropical to temperate ecosystems (Longhurst, 1998). However, current information covering phytoplanktonic communities from the Mozambican coastal region is still very scarce and inhomogeneous.

* Corresponding author.
E-mail address: cgsa@fc.ul.pt (C. Sá).
[1] Present address: Departamento de Biologia & CESAM, Universidade de Aveiro, Campus Universitário de Santiago, Aveiro, Portugal.

1385-1101/$ – see front matter © 2013 Elsevier B.V. All rights reserved.
http://dx.doi.org/10.1016/j.seares.2013.01.001

One way of assessing the phytoplankton community structure at the class level is through pigment analysis, as certain key pigments are exclusive of some phytoplankton groups (Jeffrey et al., 1997). This method is widely used in oceanographic studies and has been applied in some of the few studies conducted in Mozambique focused off the Delagoa Bight, Maputo Bay and Sofala Bank (Barlow et al., 2007, 2008; Kyewalyanga et al., 2007; Leal et al., 2009). Unfortunately, pigment information is insufficient to provide detailed information to derive the species level. In contrast, microscopic analysis is a time-consuming and crucial method for the identification of key species, such as ecological-indicators or species with potential ecological implications (e.g., toxic species). When combined, these two methods provide a powerful tool to improve our knowledge on phytoplankton communities and their dynamics (Silva et al., 2008; Wright and Jeffrey, 2006).

The Mozambique Ecosystem Survey of the Nansen EAF Programme in 2007 was an opportunity to contribute to the knowledge of this region and to study the phytoplankton communities along a wide latitudinal gradient. Our program focus was to discover new insights on the phytoplankton assemblages of the coastal region of Mozambique by addressing the following questions: Are there any latitudinal differences in phytoplankton abundance and community composition? How do the physico-chemical properties of the medium relate with eventual differences observed? What species are present along the coast? The present work intends to provide an assessment of phytoplankton abundance and community composition along the Mozambican coast by analyzing in situ photosynthetic pigments and complementing it with microscopic analysis. The physico-chemical properties of temperature, salinity and nutrients associated with water masses were also analyzed in order to relate variations in the phytoplankton assemblages to environmental conditions.

2. Material and methods

2.1. Sampling

Sampling was performed on board the R/V "Dr. Fridtjof Nansen" between September 30 and December 4 of 2007. CTD (salinity, temperature, depth) profiles were measured along the coast as part of the main cruise objective, the assessment of fishery resources of Mozambique. Whenever it was possible, water samples were collected using a rosette sampler, both at surface and fluorescence maximum depth (sub-surface maximum, from now on SSM) for posterior quantification of photosynthetic pigments and nutrients (Fig. 1). A total of 34 stations (68 samples: surface and SSM) were analyzed. The cruise was conducted in several legs along the coastline, completing a South–North (first phase: regions A, B1 and C1) and return (second phase: regions C2 and B2) trajectories. During the second phase of the cruise, samples from 10 of the 34 stations were also collected (15 samples: 10 at surface and only 5 at SSM) for microscopic analysis of phytoplankton specific composition (in white, Fig. 1). All analyses were performed at the Center of Oceanography of University of Lisbon, Portugal.

2.2. Nutrient analysis

Water samples were collected and immediately frozen for posterior nutrient analysis. Nutrients were determined through colorimetric analyses with a Tecator FIAstar™ 5000 Analyser. Nitrite (NO_2^-), nitrate (NO_3^-), phosphates (PO_4^{3-}, hereafter referred to as P), and silicates ($Si(OH)_4$, hereafter referred to as Si) were determined according to Grasshoff (1976), Bendschneider and Robinson (1952), Murphy and Riley (1962), and Fanning and Pilson (1973), respectively. As water properties from this region are typically oligotrophic (Lutjeharms, 2006), the nitrite and nitrate sum were used ($NO_2^- + NO_3^-$, hereafter referred to as N). Detection limits of the methods are 0.1 μM for P, 0.11 μM for N, and 0.5 μM for Si.

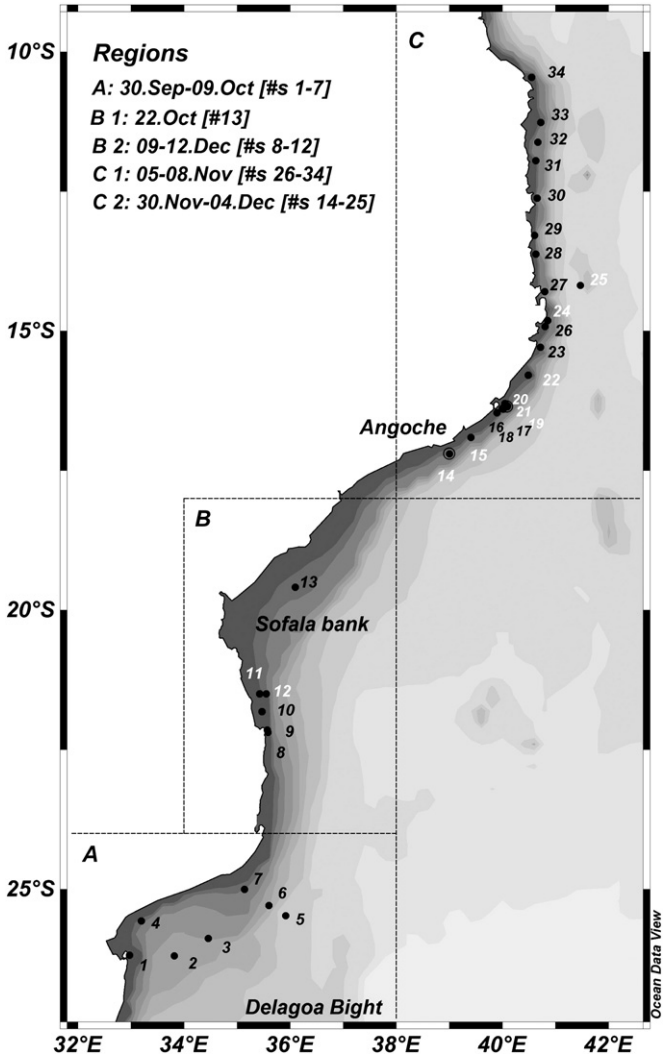

Fig. 1. Location of collected samples for determination of photosynthetic pigments (HPLC) and nutrients. Stations in white were also sampled for microscopic analysis.

2.3. Phytoplankton analyses

Phytoplankton samples were preserved with hexamethylenetetramine buffered formalin to a final concentration of 2% (Throndsen, 1978). Phytoplankton species were identified and enumerated in subsamples of 100 mL by the Utermöhl technique (Hasle, 1978), using a Zeiss Axiovert 200 inverted microscope with phase contrast and bright field illumination. A magnification of 200× was used to analyze the phytoplankton assemblage with a detection limit of 50 cells L^{-1}. Whenever possible, the cells were identified to species level according to Tomas (1997) and Hoppenrath et al. (2009). To complete the identification of the coccolithophore assemblage, each sample was filtered through a 47 mm nitrate cellulose membrane (Whatman) with a 0.45 μm nominal pore size and observed with scanning electron microscope (JEOL-5000). Species were identified following Young et al. (2003).

The observed cells were counted and organized in four groups: diatoms, dinoflagellates, coccolithophores and others. This last group included all identified and non-identified species attributable to Chrysophyceae, Cyanophyceae, Chlorophyceae, or ciliates.

2.4. Pigments

For HPLC pigment analysis, 2 L of seawater was immediately filtered through glass fiber filters (25 mm ∅ and 0.7 μm pore — Whatman GF/F). Filters were immediately frozen on board at −20 °C and stored, at

arrival of each leg, in −80 °C until analysis. For pigment analysis, filters were extracted with 3 mL of 95% cold-buffered methanol (2% ammonium acetate) for 30 min at −20 °C in the dark. Samples were sonicated (Bransonic, model 1210) for 1 min at the beginning of the extraction period, centrifuged at 1100 *g* for 15 min, at 4 °C and extracts filtered (Fluoropore PTFE filter membranes, 0.2 μm pore size) for injection in the HPLC. Pigment extracts were analyzed using a Shimadzu HPLC comprised of a solvent delivery module (LC-10ADVP) with system controller (SCL-10AVP), a photodiode array (SPD-M10ADVP), and a fluorescence detector (RF-10AXL). The chromatographic separation of pigments was achieved using the method described in Zapata et al. (2000), which uses a monomeric OS C8 column and a mobile phase constituted by two solutions: methanol:acetonitrile:aqueous pyridine and methanol: acetonitrile:acetone; a flow rate of 1 mL.min^{-1} and a run duration of 40 min. Pigments were identified from absorbance spectra and retention times, and concentrations calculated from the signals in the photodiode array detector. The limit of detection (LOD) and limit of quantification (LOQ) of this method were calculated and are discussed in Mendes et al. (2007). The HPLC system was calibrated with pigment standards from Sigma (Chl *a*, *b* and β-carotene) and DHI (for other pigments).

The assessment of phytoplankton community composition was based on size class classification from pigment concentration. Categorization of phytoplankton by size has been conventionally defined by marine biologists as: picoplankton (<2 μm in diameter), comprising pico-prokaryotes (cyanobacteria, prochlorophytes and other bacteria) and pico-eukaryotes; nanoplankton (2–20 μm), eukaryotic flagellates (cryptophytes, chrysophytes, prymnesiophytes and chlorophytes); and microplankton (20–200 μm), diatoms and dinoflagellates (Aiken et al., 2009).

Size-classes were here calculated using the method proposed by Vidussi et al. (2001), in which the fraction of each size class is given by the ratio of diagnostic pigments characteristic of the algal groups contributing to that size class versus the sum of all diagnostic pigments considered, using the coefficients proposed by Uitz et al. (2006). According to this method, the total Chl *a* can be recreated from the expression $C = \sum DP_w$, where $\sum DP_w$ is the sum of the seven selected diagnostic pigments, weighted with respect to the total chlorophyll *a* concentration and is described as following:

$$\sum DP_w = 1.41\,[\text{Fuco}] + 1.41\,[\text{Perid}] + 1.27\,[\text{Hexa}-\text{Fuco}] + 0.35\,[\text{Buta}-\text{Fuco}] + 0.6\,[\text{Allo}] + 1.01\,[\text{TChl}\,b] + 0.86\,[\text{Zea}]. \quad (1)$$

These coefficients were obtained from a global pigment database and applied in regional studies. For instance, Barlow et al. (2011) used it to characterize phytoplankton community off Tanzania. In the present study, linear regression analysis proved that the weighted sum of the seven diagnostic pigments was a valid estimate for biomass for both surface (r^2: 0.94, n = 34, p<0.01) and SSM (r^2: 0.98, n = 34, p<0.01) samples. Biomass was determined as total chlorophyll *a* concentration (TChl *a*), estimated as the sum of monovinyl chlorophyll *a*, divinyl chlorophyll *a*, chlorophyllide *a*, and chlorophyll *a* allomers and epimers.

After $\sum DP_w$ calculations, the fractions (f) of each size class are then calculated applying the following expressions:

$$f_{micro} = (1.41[\text{Fuco}] + 1.41[\text{Perid}])/\sum DP_w \quad (2)$$

$$f_{nano} = (1.27[\text{Hexa}-\text{Fuco}] + 0.35[\text{Buta}-\text{Fuco}] + 0.6[\text{Allo}])/\sum DP_w \quad (3)$$

$$f_{pico} = (1.01\,[\text{TChl}\,b] + 0.86\,[\text{Zea}])/\sum DP_w. \quad (4)$$

It should be mentioned that these size-classes calculations are general approximations, as some of the pigments can be present in more than one group and some groups can span through more than one size class (Uitz et al., 2006; Vidussi et al., 2001). For instance, fucoxanthin is a major pigment in diatoms (included in the micro-sized phytoplankton) that can be also present in prymnesiophytes and chrysophytes (included in the nano-sized phytoplankton). Microscopy results, however, reinforced the use of fucoxanthin as a marker pigment for diatoms in this study as fucoxanthin revealed strong correlation with microscopy observations (r^2: 0.93; n = 15, p<0.05). This correlation was strengthened by the fact that one station with no fucoxanthin revealed no diatoms under the microscope, but only flagellates, such as prymnesiophytes (coccolithophores). Furthermore, this pigment did not correlate with Hexa or Buta (r^2: 0.08 and r^2: 0.001; n = 68, p<0.01), which are marker pigments for prymnesiophytes and chrysophytes.

For comparison with microscopy results, micro- and nano-size indices were assumed to sum one hundred percent, as pico-sized phytoplankton are not expected to be observable under the microscope. Microscope observations of nano-sized phytoplankton were considered as the sum of coccolithophores and others (small non-identified species), and the micro-sized index as the sum of diatoms and dinoflagellates. Although peridinin pigment was not detected in any of the samples taken along the coast, suggesting that peridin-containing dinoflagellates were absent or its concentration was below detection limit, microscopic analysis revealed the presence of dinoflagellates, mostly of small size (non-identified species). Both micro and nano-sized-classes were verified to be correlated with cell counting microscopy (r^2 = 0.90, n = 15, p<0.01).

Regarding the pico-sized group, prochlorophytes could be further identified as DvChl *a* was quantified and it is an exclusive pigment of this group.

2.5. Statistical analysis

One-way ANOVA test was carried out using STATISTICA10 software in order to evaluate the statistical significance of observed differences in phytoplankton community. Multiple comparisons among pairs of variables were performed using the Tukey test, when a significant difference was found with ANOVA (p<0.05). Correlation between phytoplankton groups and biomass was investigated using the Pearson-correlation test. Data were tested previously for normality and homogeneity of variance. Parametric tests were conducted when appropriate.

Using PRIMER6 software (Clarke and Gorley, 2006), phytoplankton community structure distribution was investigated through a Cluster analysis based on the Bray–Curtis similarity method. The mean relative contribution of the different groups to that structure was further analyzed with Similarity Percentage procedure (SIMPER).

A Canonical Correspondence Analysis (CCA) was performed to investigate the effects of environmental variables on the distribution of the phytoplankton community. Water temperature, salinity, bottom depth, TChl *a* (biomass proxy) and nutrient concentrations (Si, P and N) were the environmental variables included in the CCA to retrieve their relation to phytoplankton groups' distribution. The CCA was performed using CANOCO 4.5 (Ter Braak and Smilauer, 2002). In order to evaluate the significance of the CCA results, a Monte Carlo permutation test was included in the analysis.

3. Results

3.1. Oceanographic conditions and nutrient concentrations

A North–South gradient of temperature and salinity was observed, as well as contrasting cruise-phase conditions (Fig. 2; Table 2). During the first sampling phase, the surface temperature registered off the southern coast was below 25 °C and salinity around 35.5 (Fig. 2a, c). Conversely, in the northern coast, which was sampled during early November, higher surface temperatures (>26 °C) and relatively lower salinities (~35) were observed (Fig. 2a, c). Temperature increased (>28 °C) during the second sampling phase, in late November and early December (Fig. 2b), while a decrease in salinity was observed for

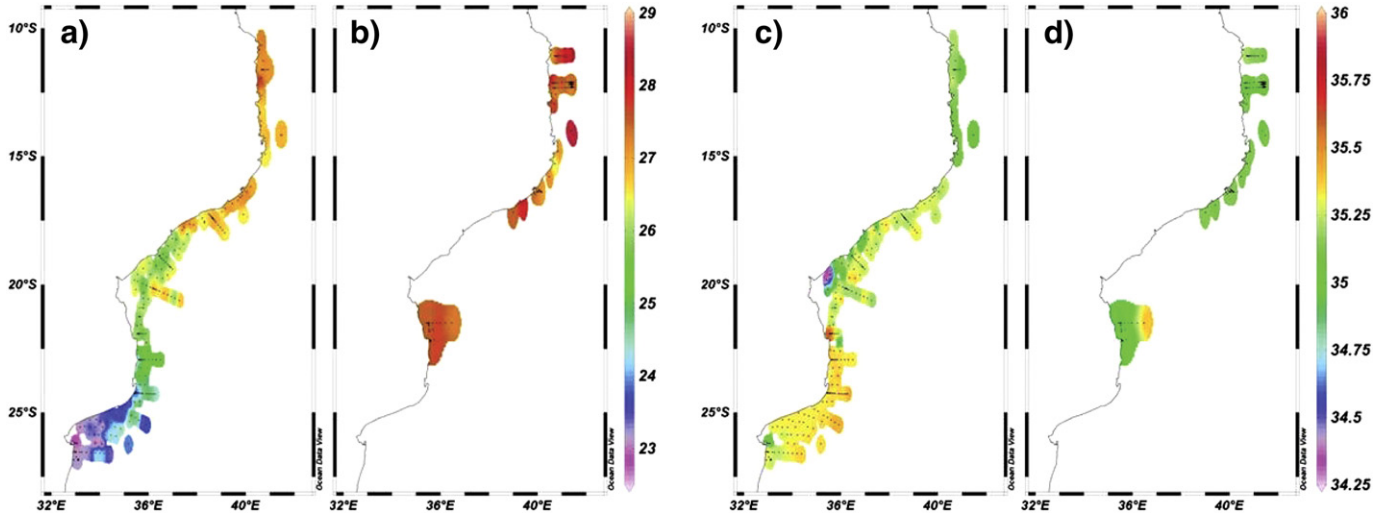

Fig. 2. Surface spatial distribution of temperature (°C), in phase 1 (a) and phase 2 (b), and salinity in phase 1 (c) and phase 2 (d).

the same period (Fig. 2d). Besides the latitudinal gradient observed for both temperature and salinity, the only region that revealed a noteworthy difference on salinity data was Sofala Bank (Fig. 2c; region B). Less saline (~34) surface waters were observed (Fig. 2a, c) in this area in the center of Mozambique. Average CTD profiles for each area revealed generally mixed waters for regions A and C2, and more stratified waters for regions B and C1. Stratification in region C1 is less pronounced with a deeper thermocline than region B (data not shown).

Nutrient results revealed similar P concentrations in all regions (~0.25 μM), with minimum values observed in region C1 (Fig. 3). Maximum Si concentration was observed in station 3 (17.27 μM) and generally varied between 6 and 10 μM in all other stations, except for occasional minima and region B, where results were below detection limit. N concentrations were generally low along the coast, often below detection limit. In contrast, higher concentrations were particularly observed in few surface samples in regions A and C1 (Fig. 3). No clear trend or differences in nutrient concentrations were observed between surface and SSM samples.

3.2. Phytoplankton assemblages

3.2.1. Biomass and pigments

Total Chl *a* averaged results revealed Delagoa Bight (region A) and Sofala Bank (region B) as the most productive areas (Table 1). For region A, values of TChl *a* ranged from 0.09 to 1.6 μg L^{-1} (Table 1) and a notable inshore–offshore gradient was observed. Lower values were associated with the deep-outermost stations (#5 and #6) while higher values were observed in the coastal stations (Fig. 4). This gradient was also observed for DvChl *a*. For region B, TChl *a* ranged from 0.18 to 0.9 μg L^{-1} (Table 1) and no DvChl *a* was detected (Table 1, Fig. 4). The lowest TChl *a* concentrations were registered in region C, where similar values were found at surface and SSM for regions C1 (0.11 μg L^{-1}). Contrastingly, C2 region evidenced a biomass increase at SSM where the maximum values reached once 0.95 μg L^{-1}. DvChl *a* concentration values were, however, higher for region C1 (Table 1, Fig. 4), namely at SSM.

Pigment information was further used to calculate size-class indices: micro-, nano- and pico-sized phytoplankton, as described in Section 2.4,

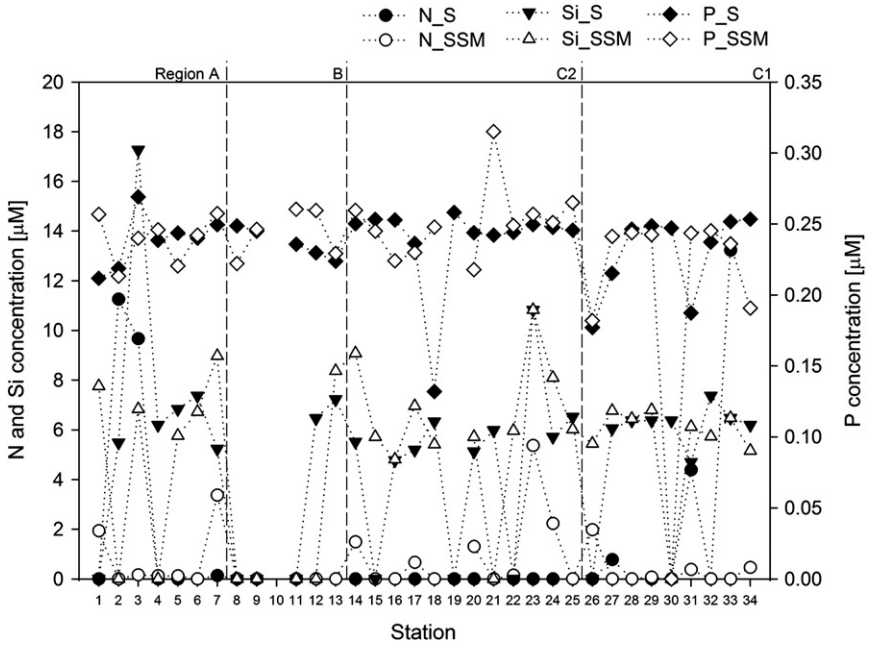

Fig. 3. Nutrient concentrations: nitrate + nitrite, N; silicates, Si; and phosphates, P at the surface (S) and at sub-surface maximum (SSM) of the sampled stations.

Table 1
HPLC pigment concentrations (μg L^{-1}) for each area and their associated phytoplankton classes (Jeffrey et al., 1997). At surface (surf.) and sub-surface maximum (SSM). Pigment concentration is set to "0" when pigment was below detection limit, and "–" when was not detected.

Pigment	Abb.	Depth	Average (minimum–maximum) concentration (μg L^{-1}) per region				Occurrence
			A	B	C1	C2	
Chlorophyll *a*	Chl *a*	Surf.	0.65 (0.05–1.6)	0.33 (0.18–0.53)	0.11 (0.03–0.34)	0.09 (0.01–0.44)	A proxy of total algae biomass
		SSM	0.72 (0.21–1.62)	0.43 (0.2–0.86)	0.12 (0.07–0.27)	0.24 (0.03–0.95)	
Divinyl chlorophyll *a*	DvChl *a*	Surf.	0.05 (0–0.15)	–	0.01 (0–0.03)	0.006 (0–0.03)	*Prochlorococcus* sp.
		SSM	0.08 (0–0.16)	–	0.04 (0–0.07)	0.005 (0–0.04)	
Total chlorophyll *a* (Chl *a* + DvChl *a*)	TChl *a*	Surf.	0.7 (0.09–1.6)	0.33 (0.18–0.53)	0.12 (0.03–0.37)	0.10 (0.03–0.44)	A proxy of total algae biomass
		SSM	0.8 (0.3–1.62)	0.43 (0.2–0.86)	0.17 (0.09–0.31)	0.24 (0.03–0.95)	
Chlorophyll *b*	Chl *b*	Surf.	0.06 (0–0.13)	0.02 (0.01–0.04)	0.02 (0–0.06)	0.006 (0–0.02)	Chlorophytes, euglenophytes,
		SSM	0.09 (0.03–0.12)	0.03 (0.02–0.04)	0.06 (0.04–0.08)	0.02 (0–0.04)	and prasinophytes
Chlorophyll *c*3	Chl *c*3	Surf.	0.11 (0–0.42)	0.006 (0–0.04)	0	0.009 (0–0.05)	Chrysophytes and prymnesiophytes
		SSM	0.13 (0–0.51)	0.04 (0–0.18)	0	0.03 (0–0.23)	
Chlorophyll *c*1 + *c*2	Chl *c*1,	Surf.	0.08 (0–0.29)	0.03 (0–0.06)	0	0.009 (0–0.05)	Diatoms, prymnesiophytes, chrysophytes,
	*c*2	SSM	0.08 (0–0.25)	0.03 (0–0.08)	0	0.03 (0–0.23)	and dinoflagellates
Fucoxanthin	Fuco	Surf.	0.26 (0–0.99)	0.18 (0.06–0.3)	0.01 (0–0.05)	0.06 (0–0.25)	Diatoms, prymnesiophytes, and chrysophytes
		SSM	0.3 (0–0.96)	0.22 (0.08–0.4)	0.02 (0–0.05)	0.13 (0–0.55)	
19′ Hexanoyloxyfucoxanthin	Hexa	Surf.	0.07 (0–0.14)	0.05 (0.04–0.08)	0.02 (0–0.07)	0.02 (0.005–0.05)	Prymnesiophytes
		SSM	0.09 (0.03–0.13)	0.04 (0.03–0.06)	0.06 (0.03–0.06)	0.02 (0–0.06)	
19′ Butanoyloxyfucoxanthin	Buta	Surf.	0.02 (0–0.09)	0.004 (0–0.01)	0	0.001 (0–0.008)	Chrysophytes and prymnesiophytes
		SSM	0.04 (0–0.07)	0	0.02 (0–0.04)	0.003 (0–0.01)	
Alloxanthin	Allo	Surf.	0.001 (0–0.002)	0	0 (0–0.001)	0	Cryptophytes
		SSM	0.001 (0–0.003)	0	0	0 (0–0.001)	
Zeaxanthin	Zea	Surf.	0.1 (0.02–0.16)	0.08 (0.07–0.11)	0.07 (0.03–0.19)	0.05 (0.009–0.11)	Cyanobacteria and chlorophytes
		SSM	0.08 (0.04–0.12)	0.07 (0.02–0.13)	0.04 (0.02–0.08)	0.02 (0.007–0.05)	
β,β-Carotene	β-car	Surf.	0.009 (0–0.02)	0.002 (0–0.009)	0	0	
		SSM	0.01 (0–0.04)	0	0	0	

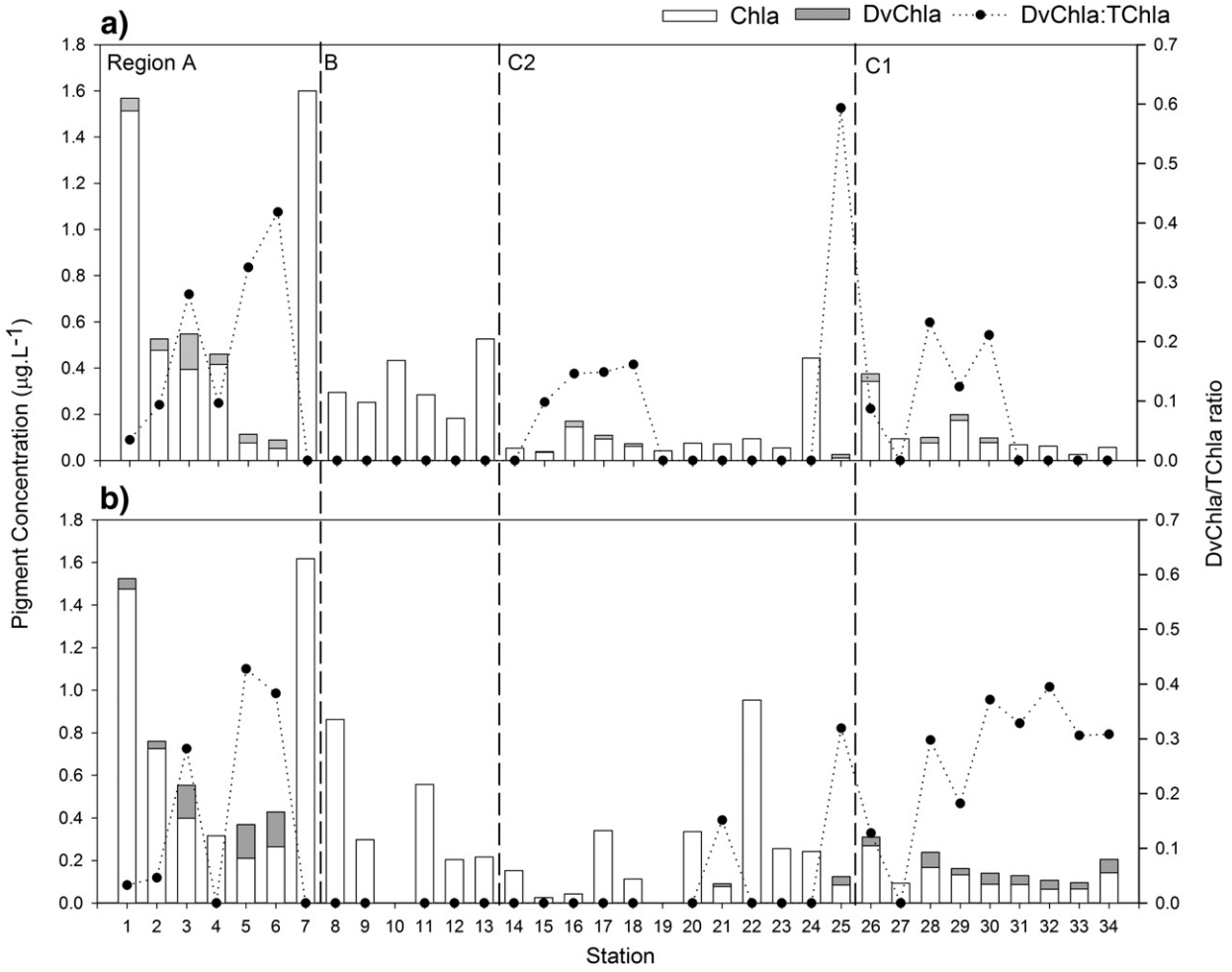

Fig. 4. Chlorophyll *a* (Chl *a*) and divinyl chlorophyll *a* (DvChl *a*) concentrations (μg L^{-1}), empty and full columns, respectively, for all the collected samples. Dots represent the ratio between DvChl *a* and the total chlorophyll *a* (TChl *a* = Chl *a* + DvChl *a*) concentrations. (a) For surface samples and (b) for SSM samples.

for characterizing phytoplankton community structure in the sampled regions (Fig. 5). Delagoa Bight area (region A) showed a clear difference between coastal and offshore stations, as well as differences in community structure with depth (Fig. 5a and b). Micro- and nanophytoplankton dominated coastal stations, mainly at SSM. In contrast, the northerner offshore stations (#5 and 6) were dominated by a picophytoplanktonic community at surface, which was altered by the presence of nano-sized phytoplankton with depth (SSM samples). This change in the community composition was also observed in all stations dominated at surface by picophytoplankton in C1 region. Micro-sized phytoplankton were weakly represented in this area, but were a relevant group to biomass on regions C2 and B. When present at surface this size-class increased its contribution to biomass with depth (SSM samples). Biomass values (TChl *a*) were significantly correlated to micro and nano-phytoplankton indices (Pearson correlation test, $p<0.05$). Contrastingly, pico-sized phytoplankton were inversely correlated with biomass. One-way ANOVA results showed significant differences in community structure with depth ($p<0.05$). Tukey tests revealed pico-sized class associated with surface samples.

Statistical similarity between stations ($p<0.05$), for both surface and SSM, was investigated through cluster analyses based on the relative contribution of each phytoplankton size-class. Three main groups were identified when analyzing a 70% similarity, which are represented in Fig. 6 as gray diamonds, black triangles and white triangles. SIMPER analysis of surface samples revealed a first cluster of stations (gray diamonds), where microphytoplankton were the main group contributing to cluster similarity. Stations included in this cluster were generally grouped together when analysis was performed at SSM. The two other main groups identified (triangles in Fig. 6) were characterized, at surface, by pico-sized phytoplankton, with no contribution of micro- or nanophytoplankton for the black cluster. Stations of these two clusters were also grouped together at SSM, however with differences in community similarity contribution. White cluster stations maintained pico-sized phytoplankton as the main contributor (~50%), while the black cluster presented co-dominance of both pico and nano-sized classes (Fig. 6). Only one station (black circle) was not grouped within these three clusters.

The role of several parameters on the distribution of the different phytoplankton size-classes was evaluated through a CCA. The Monte Carlo test showed that the variables selected (salinity, temperature, bottom depth, TChl *a*), and nutrients (N, P and Si) significantly contributed ($p<0.002$) to explain the spatial distribution of the phytoplankton size-classes (Fig. 7). CCA analysis separated surface samples (full symbols, Fig. 7) from the SSM samples (empty symbols, Fig. 7). Surface samples were associated with micro- and pico-sized phytoplankton and higher P concentrations, whereas SSM samples were associated with nano-sized phytoplankton. The surface northern stations (region C) were related to higher temperatures as opposed to samples in regions A and B (at both depths). Coastal stations (regions A and B) with higher TChl *a* and lower Si were grouped with micro-size index, while deeper stations (higher "bottom_depth") were associated with the pico-size index (region C).

3.2.2. Microscopic analysis

Although samples for microscopic analysis were only available in the second phase of the cruise, there is at least one sample from the three main cluster groups identified for both surface and SSM (Table 3). No diatoms and 90% dominance of coccolithophores were observed at surface samples from the black cluster. The most abundant genera/species were *Discosphaera tubifera* and *Acanthoica quattrospina*. At SSM, dominance of coccolithophores decreased to 50% and contribution of small flagellates and diatoms increased. Both gray and white clusters revealed for both depths an average dominance of diatoms between 70 and 90%. The most abundant genera/species identified were *Chaetoceros* spp., *Pseudo-nitzschia* spp., *Proboscia alata*, *Cerataulina pelagica* and *Thalassionema nitzschioides*. Table 4 lists all the identified species in the samples observed ($n=15$).

4. Discussion

Delagoa Bight (region A) and Sofala Bank (region B) areas were the most productive areas sampled, as previously observed by Mordasova (1980) in Barlow et al. (2008) and by Quartly and Srokosz (2004), who found identical Chl *a* variation range (0.04 and 1.4 mg m^{-3}).

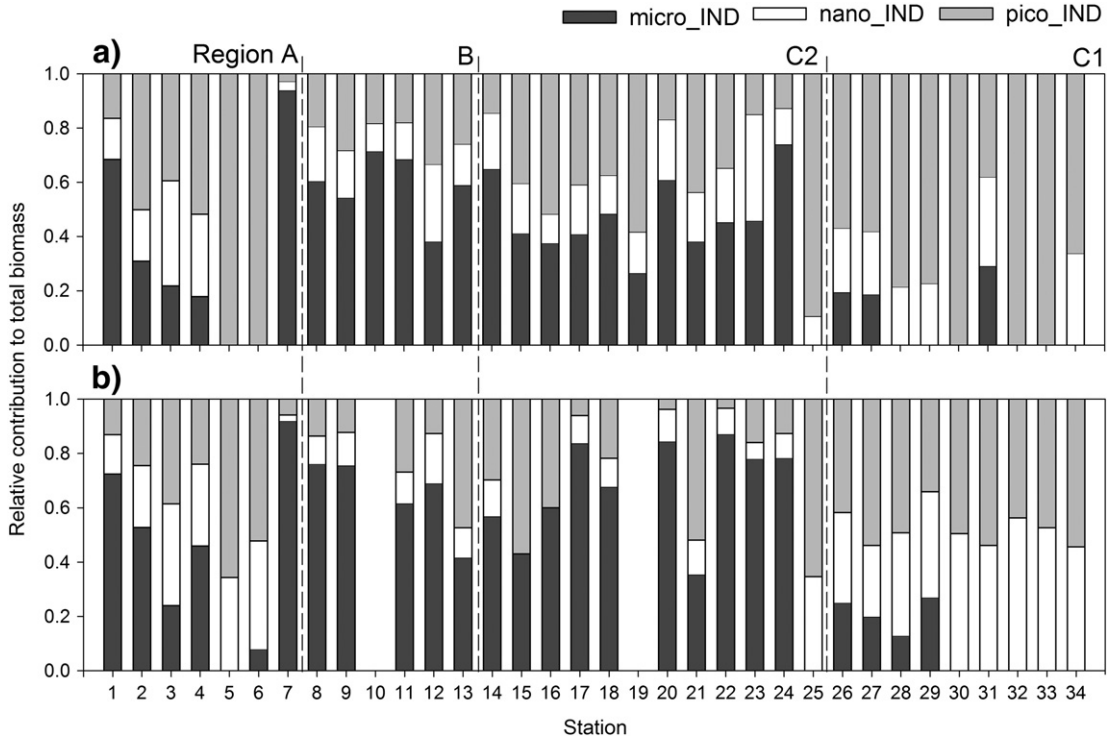

Fig. 5. Pigment indices variability at surface (a) and SSM (b). Micro-, nano-, and pico-sized indices in dark, white and light gray columns, respectively.

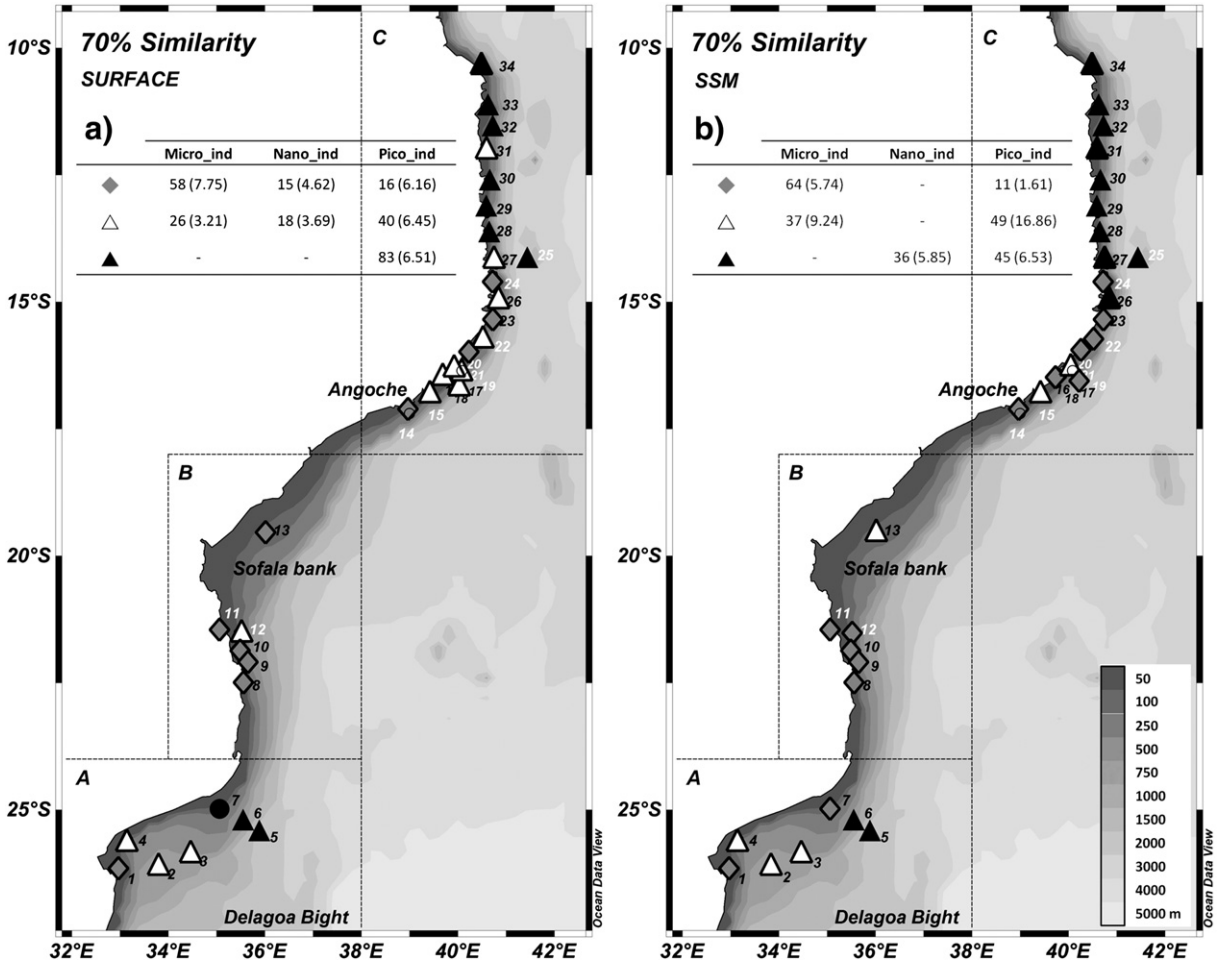

Fig. 6. Map representing 70% similarity between samples phytoplankton size-class indices composition at surface (a) and at SSM (b). Each station is represented by the symbol of the cluster in which they were grouped. Tables in the figure indicate the average percentage contribution of each phytoplankton size-class to the similarity, with standard deviation in parenthesis.

Delagoa Bight is a shallow shelf centered on 34°E, 26°S where a poleward flow passing this bight generates a cyclonic eddy in the region throughout most of the year (Lutjeharms and Da Silva, 1988). Upwelling associated with these eddies and current flows injects nutrients into the surface layers which, together with nutrients supplied by the Limpopo river outflow, enhances phytoplankton production in the area. The occurrence of upwelling in this area is expected to favor the growth of diatoms, which are adapted to major develop in nutrient-rich mixed waters, as it was observed in the inner shore stations. Results evidence, however, nitrate depletion, as most stations showed concentrations below the limit of detection. Barlow et al. (2008) also reported very small nitrate values for Delagoa Bight. This depletion is probably associated to the prompt consumption of nutrients by diatoms, which is also supported by the presence of higher Si concentrations where this group is less abundant (Fig. 7). Silica values retrieved during this study were in accordance to the average concentration of 8.857 μmol L^{-1} reported by other authors for the western Indian Ocean (WIO) (Barlow et al., 2008; Leal et al., 2009; Paula et al., 1998). Nutrients have been identified as controllers of phytoplankton biomass growth for the WIO, with nitrogen playing a key role and therefore determining phytoplankton abundance and composition (Kyewalyanga et al., 2007; Leal et al., 2009; Lutjeharms and Da Silva, 1988). A shift to pico-size-dominant community was observed for the offshore warmer waters with lower biomass (Fig. 4), namely *Prochlorococcus*, as evidenced by the presence of DvChl *a* pigment. This group is adapted to survive in these oceanic nutrient-poor waters (Bouman et al., 2011).

The Sofala Bank area (region B) is acknowledged as an important fishery ground, as biomass distribution is generally associated with nutrient input from the Zambezi river runoff. This is closely related to rainfall events and oceanographic currents' heterogeneity on the mid-continental shelf waters (Leal et al., 2009). Salinity is known to

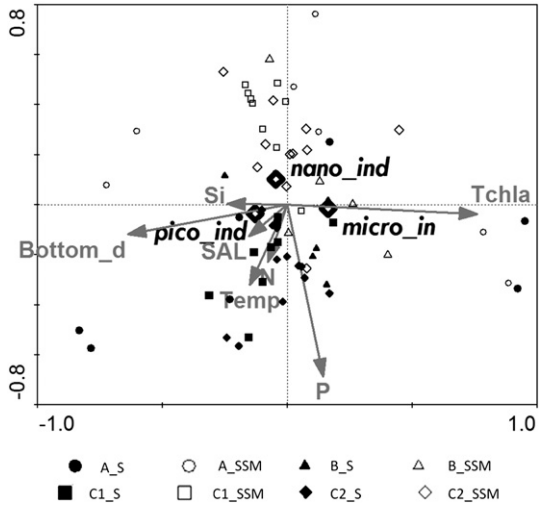

Fig. 7. Canonical Correspondence Analysis ordination diagram relative to data on contribution of phytoplankton size-classes. Arrows refer to total biomass (T_Chl *a*) and environmental variables (water temperature (temp), salinity (SAL), bottom depth (bottom_d), dissolved inorganic nitrogen (N), phosphate (P) and silicate (Si). Diamonds ( ) refer to phytoplankton size-class indices (*Micro_ind*, micro-; *Nano_ind*, nano-; *Pico_ind*, pico-sized phytoplankton).

Table 2
Environmental data table.

	Average (minimum–maximum) per region				
	A	B1	B2	C1	C2
Nr of stations	7	1	5	9	12
Bottom depth (m)	617 (41–1530)	39	103 (45–228)	134 (44–206)	94 (17–431)
Depth of SSM (m)	50 (15–88)	30	30 (23–40)	53 (31–83)	30 (15–90)
Surface					
Temperature (°C)	23.5 (22.8–24.7)	25.9	27.5 (27.3–27.8)	27.0 (26.5–28.2)	27.6 (26.5–28.5)
Salinity	35.3 (35.1–35.4)	34.9	34.9 (34.6–35.1)	35.2 (35.1–35.3)	35.1 (35.1–35.2)
Sub-surface maximum (SSM)					
Temperature (°C)	22.2 (21.2–22.9)	25.5	27.2 (27.1–27.4)	25.9 (25.3–26.8)	25.7 (23.7–27.9)
Salinity	35.3 (35.1–35.4)	35.0	35.2 (35.1–35.3)	35.1 (35.1–35.2)	35.1 (35.0–35.3)

vary seasonally in this area, sometimes reaching values as low as 20 (Lutjeharms, 2006). During the present study sampling took place during the dry season, and salinity values were always above 34 (Table 2). Micro-sized plankton dominated this region, in comparable amounts as coastal stations in region A (#1 and #7), (see Fig. 5). Microscopic analysis confirmed a diatom-dominated assemblage (70% contribution), where large *Chaetoceros* spp. and *P. alata* were the most abundant species (20% and 16% respectively of all diatom population). These species are usually indicative of mature upwelled waters and water column stability, confirmed by CTD profiles, and also supported by the presence of dinoflagellates. Although in this study no peridin pigment was detected, suggesting that peridin-containing dinoflagellates were absent or its concentration was below detection limit, microscopic analysis revealed the presence of small-size dinoflagellates (Table 3) mostly abundant in this area (20% contribution in region B). DvChl *a* was not detected, which indicates that *Prochlorococcus* are not expected to be part of the pico-sized phytoplankton community present in this coastal shallow region.

The lowest biomass values were retrieved in the northern stations of the coast where warmer waters were found. This north–south water temperature differences observed are in accordance with Sete et al. (2002) who, by analyzing cruises' data from 1977 to 1980, reported that year round the temperatures were higher in northern than in southern Mozambique. This feature was explained by the presence of Equatorial water mainly in the north and Subtropical water in the south. In northern Mozambique (region C), the two areas sampled revealed differences in productivity and phytoplankton size-classes dominance. Region C1 is mostly influenced by the presence of equatorial waters and was clearly dominated by a pico-sized community at surface, namely by *Prochlorococcus* (indicated by the presence of DvChl *a*). The presence of equatorial water mass in this region may favor the abundance of this group, which has a minimal cell size and the highest surface area to

Table 3
Microscopy results.

Region	Cluster	Station		Diatoms	Dinoflagellates	Coccolithophores	Others	Nr of species identified	Dominant species (sum > 50% of total counts)
Surface									
B	◆	11	[cells L^{-1}]	12,720	157	910	157	34	*Proboscia alata* [32%], *Chaetoceros* spp. [23%]
			[%]	91	1	7	1		
B	△	12	[cells L^{-1}]	2887	774	63	272	19	*Chaetoceros* spp. [21%], small dinoflagellates [18%],
			[%]	72	19	2	7		*Proboscia alata* [16%]
C	◆	14	[cells L^{-1}]	3515	188	24	31	26	*Chaetoceros* spp. [18%], *Pseudo-nitzschia* spp. [17%],
			[%]	88	5	6	1		*Cylindrotheca closterium* [10%], *Pseudo-nitzschia* spp. [9%]
C	△	15	[cells L^{-1}]	6402	199	669	21	28	*Chaetoceros* spp. [40%], *Pseudo-nitzschia* spp. [15%]
			[%]	88	3	9	0		
C	△	19	[cells L^{-1}]	7145	314	774	10	24	*Chaetoceros* spp. [57%]
			[%]	87	4	9	0		
C	◆	20	[cells L^{-1}]	10,858	481	387	0	44	*Chaetoceros* spp. [45%], *Pseudo-nitzschia* spp. [9%]
			[%]	93	4	3	0		
C	△	21	[cells L^{-1}]	6339	105	398	0	29	*Chaetoceros* spp. [38%], *Hemiaulus haukii* [8%],
			[%]	93	2	6	0		*Pseudo-nitzschia* spp. [6%]
C	△	22	[cells L^{-1}]	4205	293	994	0	29	*Chaetoceros* spp. [43%], n. ident coccolithophores [13%]
			[%]	77	5	18	0		
C	◆	24	[cells L^{-1}]	19,812	377	324	10	25	*Chaetoceros* spp. [81%]
			[%]	97	2	2			
C	▲	25	[cells L^{-1}]	0	63	575	0	5	N. ident coccolithophores [46%],
			[%]	0	10	90	0		*Discosphaera tubifera* [25%]
SSM									
B	◆	11	[cells L^{-1}]	15,597	63	544	146	21	*Chaetoceros* spp. [43%], *Pseudo-nitzschia* spp. [23%]
			[%]	95.4	0.4	3.3	0.9		
B	◆	12	[cells L^{-1}]	5345	63	418	209	23	*Proboscia alata* [72%]
			[%]	88.6	1	6.9	3.5		
		14	No sample						
		15	No sample						
		19	No sample						
C	△	21	[cells L^{-1}]	9666	42	167	0	15	*Proboscia alata* [30%], *Pseudo-nitzschia* spp. [23%]
			[%]	97.9	0.4	1.7	0		
		22	No sample						
C	◆	24	[cells L^{-1}]	17,155	157	669	0	22	*Chaetoceros* spp. [67%]
			[%]	95.4	0.9	3.7	0		
C	▲	25	[cells L^{-1}]	73	73	251	105	5	N. ident coccolithophores [42%], small flagellates [19%]
			[%]	14.6	14.6	50	20.8		

volume ratio of all marine oxygenic photoautotrophs, making them the most adapted to survive in impoverished oligotrophic environments (Bouman et al., 2011; Claustre, 1994). Barlow et al. (2007) also showed that prokaryotes dominate phytoplankton communities in the Indian Ocean, namely the prokaryote cyanobacterial *Synechococcus* sp. and *Prochlorococcus* sp. Specifically for the Mozambique Channel, the authors reported a prokaryote index > 0.7.

Under the microscope, cell counts indicated nanoplankton community as the most abundant (90% and no diatoms) in region C1, as picoplankton community is not observable with this method. The most abundant species identified were coccolithophores *D. tubifera* and *A. quattrospina*, which have been described as tracer species for warm oligotrophic waters in other oceanic basins (Andruleit et al., 2003; Boeckel and Baumann, 2008). This observation suggests that these species may be good tracers for the influence of the equatorial water mass in this region. In contrast, samples from region C2 were dominated by microphytoplankton, which is typical of cooler nutrient-rich waters. In fact, patches of cooler coastal water were observed in the SST images (data not shown), which may be related to the occurrence of oceanographic physical processes like eddies in this area (Lutjeharms, 2006). Diatom species found in this area (*Chaetoceros* spp., *Pseudo-nitzschia* sp.) are also indicative of nutrient availability and water mixing conditions (confirmed by CTD profiles).

The high productivity found in this study region has been also reported by other authors, who emphasize the major role played by the cyclonic eddies on the phytoplankton enhancement. Formation of coastal lee eddies is a consequence of the change in the direction of the coastline, and persistent and intense lee eddies have been found in offsets of the Mozambique coastline, such as in the Delagoa Bight and south of Angoche (Lutjeharms, 2007). For instance, Nehring (1987) in Lutjeharms, 2007 has shown that the highest values of Chl *a* in the channel are found in the Angoche lee eddy. Tew-Kai and Marsac (2009), who applied statistical models to satellite data (1997–2004), subdivide the central portion of the Mozambique Channel (16°S–24°S) in three sub-systems. The first one that occupies this northern part, more specifically the narrows of the channel, where eddies are at early life stages and the spin-up process of cyclonic eddies is associated with nutrient inflow in the core in the vertical plane that boosts the primary production. The second sub-system stretches out in the median part characterized by eddies becoming mature as they move along the west coast and the third subsystem located in the South part, where eddies enter a spinoff process with decreasing energy and phytoplankton growth is much reduced. Although, their study was centered in the open waters of the Mozambique Channel, they also report higher Chl *a* concentrations in coastal regions, greater by one order of magnitude than the ones found in open ocean areas. Strongest responses in the Central part were located along the Western shelf of the narrow section of the Channel (16°S–17°S) and off Sofala Bank (19°S–21°S), the same productive areas (regions B and C2) identified in the present study. Two major sources of productivity enhancement are identified: run-offs of the Zambezi, and the mesoscale eddies passing in the west part of the channel (Tew-Kai and Marsac, 2009).

Overall, results of the present study reveal both longitude (coast–offshore) and latitudinal differences. Coastal–off-shore differences were mainly seen in region A, where more productive waters were found near the coast, while latitudinal differences revealed a general increase in biomass from North to South (Fig. 4). However, the latitudinal pattern observed has to be viewed with care due to the time span of the sampling period (Oct–Dec). A synoptic view provided by satellites would be more appropriate in this sense. The temporal signal is emphasized by Tew-Kai and Marsac (2009), who conclude that both northern (10°S–16°S) and southern (24°S–30°S) regions are dominated by a seasonal signal, whereas the variability in the central region (16°S–24°S) is driven by mesoscale dynamics.

Geographically, biomass values reported here for the Mozambique coast are within the ranges found for other areas of the Indian Ocean. For instance, in a study in the adjacent coast of Tanzania, Chl *a* concentration ranged between 0.3 and 0.8 μg L^{-1} and the genera of diatoms found (e.g. *Chaetoceros* spp., *Leptocylindrus* spp. and *Pseudo-nitzschia* spp.) are among the same reported in our study (Table 4) (Lugomela et al., 2001). Barlow et al. (2011), also reported <1 μg L^{-1} Chl *a* levels for the Tanzania shelf region in a cruise performed during Sep–Oct 2007, and pigment data suggested diatoms as a major component of the communities. In contrast, Mengesha et al. (1999) reported for the Kenyan coast a very oligotrophic environment with a picophytoplankton dominated community. The oligotrophic conditions in their study area and in the northern central Indian Ocean contrast with the seasonally very productive provinces of the Somalia upwelling (Koning et al., 2001), where the upwelling period was characterized by the successive dominance of three diatom species, *T. nitzschioides*, *Nitzschia bicapitata* and *Chaetoceros* spp. resting spores. Oligotrophic conditions were also

Table 4
List of species identified through microscopic analysis.
(* for species only observed at sub-surface maximum depth).

Bacillariophyceae	Dinophyceae	
Achnanthes spp.	*Alexandrium* spp.	*Syracolithus* sp. Type A
*Asteromphalus heptactis**	*Amphidoma caudatum**	*Syracosphaera corolla*
Bacteriastrum furcatum	*Amphidinium* spp.	*Syracosphaera noroitica*
Bacteriastrum hyalinum	*Ceratium furca*	*Syracosphaera pulchra*
Bacteriastrum spp.	*Ceratium fusus**	*Syracosphaera pulchra* HOL *oblonga* type
Cerataulina pelagica	*Ceratium kofoidii**	*Syracosphaera pirus*
Chaetoceros spp.	*Ceratium massiliense**	*Syracosphaera* spp.
Cocconeis spp.	*Ceratium teres*	*Umbelosphaera irregularis*
Corethron criophilum	*Ceratium tripos*	*Umbelosphaera tenuis* type I
Coscinodiscus spp.	*Diplopsalis* sp.	*Umbilicosphaera foliosa*
Cylindrotheca closterium	*Gonyaulax spinifera*	*Umbilicosphaera sibogae*
Climacodinium fraundfeldianum	*Gymnodinium sanguineum**	*Umbilicosphaera hulburtiana*
Dactyliosolen fragilissimus	*Gymnodinium* spp.	
Detonula pumila	*Gyrodinium fusiforme*	Chrysophyceae
Ditylum brightwellii	*Gyrodinium* spp.	*Dictyocha fibula*
Eucampia zodiacus	*Ostreopsis* spp.	*Octotys octanaria*
Fragilaria spp.	*Oxytoxum* spp.	
Guinardia cf. *delicatula*	*Pronoctiluca pelagica*	Cyanophyceae
Guinardia flaccida	*Pronoctiluca spinifera*	*Oscillatoria* sp
Guinardia cf. *striata*	*Prorocentrum triestinum*	
Hemiaulus haukii	*Protoperidinium bipes*	Others
Hemiaulus sinensis	*Protoperidinium ovum**	*Myrionecta rubra*
Lauderia annulata	*Protoperidinium pellucidum*	
Leptocylindrus danicus	*Protoperidinium* spp.	
Leptocylindrus minimus		
Meuniera membranacea	Prymnesiophyceae	
Odontella mobiliensis	*Acanthoica quattrospina*	
*Planktoniella sol**	*Anacanthoica acanthos*	
Pleurosigma spp.	*Algirosphaera robusta*	
Podosira spp.	*Calcidiscus leptoporus*	
Proboscia alata	*Calcidiscus quadriperforatus*	
Pseudo-nitzschia spp.	*Calyptrolithina multipora*	
*Rhizosolenia robusta**	*Discosphaera tubifera*	
Rhizosolenia setigera	*Emiliania huxleyi* type A	
Rhizosolenia styliformis	*Emiliania huxleyi* type B	
Rhizosolenia spp.	*Emiliania huxleyi* var. *corona*	
Skeletonema costatum	*Gephyrocapsa ericsonii*	
Striatella unipunctata	*Gephyrocapsa oceanica*	
Thalassionema fraunfeldii	*Helladosphaera cornifera*	
Thalassionema nitzschioides	*Ophiaster formosus*	
*Thalassiosira subtilis**	*Ophiaster hydroideus*	
Thalassiosira spp.	*Palusphaera* sp.	
Thalassiothrix mediterranea	*Polycalyptra gaarderiae*	
Thalassiothrix spp.	*Polycrater galapagensis*	

found by Not et al. (2008) in the open ocean of the Arabian Sea, where picoplankton reached 92% contribution to phytoplanktonic biomass. In Southern Indian Ocean, Schlüter et al. (2011), who measured total Chl *a* concentrations from 0.043 to 0.083 μg L^{-1}, found coccolithophores *Emiliania huxleyi* and *Gephyrocapsa oceanica* to constitute an important part of the phytoplankton population, particularly in the SW Indian Ocean, where this group tended to dominate in surface waters. The coccolithophores species we found for the southern Mozambique coast are in accordance with this observation, and contrast with the species observed in the northern coast samples (*D. tubifera* and *A. quattrospina*). All the reported studies corroborate the spatially heterogeneity nature of the WIO and emphasize the importance of local studies to contribute for the understanding of the dynamics of this ocean as a whole.

In summary, by analyzing pigment information of samples collected along the Mozambican coast it was possible to identify latitudinal differences in the phytoplankton communities mainly related to the influence of distinct water masses in the North and South coast. Temperature was identified as the parameter related to differences observed: areas of cooler water dominated by micro-phytoplankton (diatoms) and regions of warmer water with pico-sized-dominated community. Although limited to nano- and micro-sized plankton, microscopy also allowed retrieving important information at genera and species level, which are closely related to the oceanography of the areas of appearance. Understanding biogeography of the seas is essential for ecological management and model development as shifts in community dominance are correlated to other cycles in the ecosystem. For instance, eukaryotic cells are believed to play a significant role in carbon export, whereas cyanobacteria-dominated systems tend to be more efficient at recycling carbon within the surface ocean (Corno et al. (2007) in Bouman et al., 2011). This study contributed to that knowledge as it reports invaluable in-situ data, which was unavailable for this region. The list of species and abundance patterns is also an important input to the biodiversity background knowledge of this region.

Acknowledgments

This was a special study of the "Ecosystem Survey Mozambique 2007" of the EAF Nansen Programme funded by NORAD, IMR (Bergen, Norway) and FAO. We thank Maurício Lipassula from the Eduardo Mondlane University (Mozambique) and also Drs. D. Gove and P. Santana Afonso from the Fisheries Institute of Mozambique (IIP). We also thank the crew and fellow scientists from IIP onboard the R/V "Dr. Fridtjof Nansen" and Nancy Tenenbaum for an English revision of this manuscript. Carolina Sá was funded through a grant by FCT (SFRH/BD/24245/2005) and ESA Due CoastColour. Miguel Costa Leal was funded through the project TRANSMAP (INCO-CT2004-510862) funded by the European Commission, 6th Framework. We are also thankful to two anonymous referees for helpful comments that improved this manuscript.

References

Aiken, J., Pradham, Y., Barlow, R., Lavender, S., Poulton, A., Holligan, P., Hardman-Mountford, N., 2009. Phytoplankton pigments and functional types in the Atlantic Ocean: a decadal assessment, 1995–2005. Deep-Sea Research II 56, 899–917.

Andruleit, H., Stäger, S., Rogalla, U., Cepek, P., 2003. Living coccolithophores in the northern Arabian Sea: ecological tolerances and environmental control. Marine Micropaleontology 49, 157–181.

Barlow, R., Stuart, V., Lutz, V., Sessions, H., Sathyendranath, S., Platt, T., Kyewalyanga, M., Clementson, L., Fukasawa, M., Watanabe, S., Devred, E., 2007. Seasonal pigment patterns of surface phytoplankton in the subtropical southern hemisphere. Deep-Sea Research I 54, 1687–1703.

Barlow, R., Kyewalyanga, M., Sessions, H., van den Berg, M., Morris, T., 2008. Phytoplankton pigments, functional types, and absorption properties in the Delagoa and Natal Bights of the Agulhas ecosystem. Estuarine, Coastal and Shelf Science 80, 201–211.

Barlow, R., Lamont, T., Kyewalyanga, M., Sessions, H., van den Berg, M., Duncan, F., 2011. Phytoplankton production and adaptation in the vicinity of Pemba and Zanzibar islands, Tanzania. African Journal of Marine Science 33 (2), 283–295.

Bendschneider, K., Robinson, R.J., 1952. A new spectrophotometric method for the determination of nitrite in sea water. Journal of Marine Research 11, 87–96.

Boeckel, B., Baumann, K.H., 2008. Vertical and lateral variations in coccolithophore community structure across the subtropical frontal zone in the South Atlantic Ocean. Marine Micropaleontology 67, 255–273.

Bouman, H.A., Ulloa, O., Barlow, R., Li, W.K.W., Platt, T., Zwirglmaier, K., Scanlan, D.J., Sathyendranath, S., 2011. Water-column stratification governs the community structure of subtropical marine picophytoplankton. Environmental Microbiology Reports 3 (4), 473–482.

Brunet, C., Lizon, F., 2003. Tidal and diel periodicities of size-fractionated phytoplankton pigment signatures at an offshore station in the southeastern English Channel. Estuarine, Coastal and Shelf Science 56, 833–843.

Clarke, K.R., Gorley, R.N., 2006. PRIMER v6: User Manual/Tutorial. PRIMER-E, Plymouth UK.

Claustre, H., 1994. Phytoplankton pigment signatures of the trophic status in various oceanic regimes. Limnology and Oceanography 39, 1206–1211.

De Ruijter, W.P.M., Ridderinkhof, H., Lutjeharms, J.R.E., Schouten, M.W., Veth, C., 2002. Observations of the flow in the Mozambique Channel. Geophysical Research Letters 29. http://dx.doi.org/10.1029/2001GL013714.

Fanning, K.A., Pilson, M.E.Q., 1973. On the spectrophotometric determination of dissolved silica in natural waters. Analytical Chemistry 15, 136–140.

Gove, D.Z., 1995. The coastal zone of Mozambique. Coastal Management Center conference Proceedings, pp. 251–273.

Grasshoff, K., 1976. Methods of Seawater Analysis. Verlag Chimie, New York.

Hasle, G.R., 1978. The inverted-microscope method. In: Sournia, A. (Ed.), Phytoplankton Manual. Monographs on Oceanic Methodology. UNESCO, Paris, pp. 88–96.

Hoppenrath, M., Elbrächter, M., Drebes, G., 2009. Marine phytoplankton. Selected microphytoplankton species from the North Sea around Helgoland and Sylt. Kleine Senckenberg-Reihe Band 49, Germany.

Jeffrey, S.W., Mantoura, R.F.C., Bjørnland, T., 1997. Data for the identification of 47 key phytoplankton pigments. In: Jeffrey, S.W., Mantoura, R.F.C., Wright, S.W. (Eds.), Phytoplankton Pigments in Oceanography: Guidelines to Modern Methods. Monographs on Oceanographic Methodology. UNESCO, Paris, pp. 449–559.

Koning, E., van Iperen, J.M., van Raaphorst, W., Helder, H., Brummer, G.-J.A., van Weering, T.C.E., 2001. Selective preservation of upwelling-indicating diatoms in sediments off Somalia, NW Indian Ocean. Deep-Sea Research I 48, 2473–2495.

Kyewalyanga, M.S., Naik, R., Hegde, S., Raman, M., Barlow, R., Roberts, M., 2007. Phytoplankton biomass and primary production in Delagoa Bight Mozambique: application of remote sensing. Estuarine, Coastal and Shelf Science 74, 429–436.

Leal, M.C., Sá, C., Nordez, S., Brotas, V., Paula, J., 2009. Distribution and vertical dynamics of planktonic communities at Sofala Bank, Mozambique. Estuarine, Coastal and Shelf Science 84, 605–616.

Leal, M.C., Pereira, T.C., Brotas, V., Paula, J., 2010. Vertical Migration of the Gold-spot Herring (*Herklotsichthys quadrimaculatus*) Larvae on Sofala Bank, Mozambique. Western Indian Ocean Journal of Marine Science 9, 175–183.

Longhurst, A.R., 1998. Ecological Geography of the Sea. Academic Press, London.

Lugomela, C., Wallberg, P., Nielsen, T.G., 2001. Plankton composition and cycling of carbon during the rainy season in a tropical coastal ecosystem, Zanzibar, Tanzania. Journal of Plankton Research 23 (10), 1121–1136.

Lutjeharms, J.R.E., 2006. The costal oceans of south-eastern Africa. The Sea 14, 781–832.

Lutjeharms, J.R.E., 2007. Three decades of research on the greater Agulhas Current. Ocean Science 3, 129–147.

Lutjeharms, J.R.E., Da Silva, A.J., 1988. The Delagoa Bight eddy. Deep-Sea Research 35, 619–634.

Mendes, C.R., Cartaxana, P., Brotas, V., 2007. HPLC determination of phytoplankton and microphytobenthos pigments: comparing resolution and sensitivity of a C18 and a C8 method. Limnology and Oceanography: Methods 5 (2007), 363–370.

Mengesha, S., Dehairs, F., Elskens, M., Goeyens, L., 1999. Phytoplankton nitrogen nutrition in the Western Indian Ocean: ecophysiological adaptations of neritic and oceanic assemblages to ammonium supply. Estuarine, Coastal and Shelf Science 48, 589–598.

Murphy, J., Riley, J.P., 1962. A modified single solution method for the determination of phosphate in natural waters. Analytica Chimica Acta 27, 31–36.

Not, F., Latasa, M., Scharek, R., Viprey, M., Larleskind, P., Balagué, V., Ontoria-Oviedo, I., Cumino, A., Goetze, E., Vaulot, D., Massana, R., 2008. Protistan assemblages across the Indian Ocean, with a specific emphasis on the picoeukaryotes. Deep-Sea Research I 55, 1456–1473.

Paula, J., Pinto, I., Guambe, I., Monteiro, S., Gove, D., Guerreiro, J., 1998. Seasonal cycle of planktonic communities at Inhaca Island, southern Mozambique. Journal of Plankton Research 20, 2165–2178.

Quartly, G.D., Srokosz, M.A., 2004. Eddies in the southern Mozambique Channel. Deep-Sea Research II 51, 69–83.

Schlüter, L., Henriksen, P., Nielsen, T.G., Jakobsen, H.H., 2011. Phytoplankton composition and biomass across the southern Indian Ocean. Deep-Sea Research I 58, 546–556.

Sete, C., Ruby, J., Dove, V., 2002. Seasonal variation of tides, currents, salinity and temperature along the coast of Mozambique. Relatório do Centro Nacional de Dados Oceanográficos, Unesco OdinAfrica.

Silva, A., Mendes, C.R., Palma, S., Brotas, V., 2008. Short-time scale variation of phytoplankton succession in Lisbon bay (Portugal) as revealed by microscopy cell counts and HPLC pigment analysis. Estuarine, Coastal and Shelf Science 79, 230–238.

Ter Braak, C.J.F., Smilauer, P., 2002. CANOCO Reference Manual and CanoDraw for Windows User's Guide: Software for Canonical Community Ordination (Version 4.5). Microcomputer Power, New York, USA.

Tew-Kai, E., Marsac, F., 2009. Patterns of variability of sea surface chlorophyll in the Mozambique Channel: a quantitative approach. Journal of Marine Systems 77, 77–88.

Throndsen, J., 1978. Preservation and storage. In: Sournia, A. (Ed.), Phytoplankton Manual. Monographs on Oceanic Methodology. UNESCO, Paris, pp. 69–74.

Tomas, C., 1997. Identifying Marine Phytoplankton. Academic Press Inc., London.

Uitz, J., Claustre, H., Morel, A., Hooker, S.B., 2006. Vertical distribution of phytoplankton communities in open ocean: an assessment based on surface chlorophyll. Journal of Geophysical Research 111, CO8005.
Vidussi, F., Claustre, H., Manca, B.B., Luchetta, A., Marty, J.C., 2001. Phytoplankton pigment distribution in relation to upper thermocline in the eastern Mediterranean Sea during winter. Journal of Geophysical Research 106, 19939–19956.
Wright, S.W., Jeffrey, S.W., 2006. Pigment markers for phytoplankton production. In: Volkmann, J.K. (Ed.), Marine Organic Matter: Biomarkers, Isotopes and DNA. Springer-Verlag, Berlin, pp. 71–104.
Young, J., Geisen, M., Cros, L., Kleijne, A., Sprengel, C., Probert, I., Ostergaard, J., 2003. A guide to extant coccolithophore taxonomy. Journal of Nannoplankton Research (special issue 1), 123.
Zapata, M., Rodriguez, F., Garrido, J.L., 2000. Separation of chlorophylls and carotenoids from marine phytoplankton: a new HPLC method using a reversed phase C8 column and pyridine-containing mobile phases. Marine Ecology Progress Series 195, 29–45.